PSEUDO-STATIC ANALYSIS OF PILES IN LIQUEFIABLE SOILS: PARAMETRIC EVALUATION OF LIQUEFIED LAYER PROPERTIES

Hayden J. Bowen[1] and Misko Cubrinovski[2]

SUMMARY

In this paper, pseudo-static analysis of piles in liquefying soils is applied to a case study of a bridge foundation. The response of piles is separately evaluated for the cyclic phase during the intense shaking and development of liquefaction, and for the subsequent lateral spreading phase. With regard to the considerable uncertainties involved in predicting liquefaction and lateral spreading phenomena the effects of key parameters influencing the pile response are examined through parametric analyses. Particular attention is given to the variation in stiffness and residual strength of the liquefied soil, the magnitude of lateral ground displacement and the magnitude of inertial loads from the superstructure. The results shed light on the relative importance of key parameters for different combination of loads and ground conditions, and allow comparative evaluation between loads on the pile exerted by the crust layer and the liquefied layer.

INTRODUCTION

Pile foundations are primarily designed to transfer vertical loads from the superstructure to the bearing stratum. For this reason, piles are relatively vulnerable to lateral loads such as those imposed by ground shaking during strong earthquakes. In the case of soil liquefaction, this vulnerability is particularly pronounced since the loss of strength and stiffness in the liquefied soil results in a significant loss of lateral support for the embedded piles. Soil liquefaction has caused major damage to pile foundations in previous earthquakes, particularly the 1964 Niigata (Hamada and O'Rourke 1992) and 1995 Kobe (Cubrinovski *et al.* 2001; Ishihara and Cubrinovski 1998; Ishihara and Cubrinovski 2004; Japanese Geotechnical Society 1998; Tokimatsu and Asaka 1998; Yasuda and Berrill 2000) events.

Two phases in the seismic response of piles in liquefied soil have been recognised: firstly a cyclic phase during the ground shaking and development of liquefaction, and secondly lateral spreading following the liquefaction. The soil-pile interaction in the cyclic phase is characterised by dynamic loads on the pile from both ground movements and inertial loads from the superstructure. The lateral spreading phase primarily occurs after the liquefaction has developed and is characterised by large unilateral ground displacements and relatively small inertial effects. During this phase the stiffness and strength of liquefied soils are very low, reflecting features of a completely liquefied soil.

The phenomenon of soil liquefaction and lateral spreading is complex and predictions of the seismic response of piles in liquefied soil are subject to a high level of aleatoric uncertainty. This suggests that when simplified analysis is performed, the key consideration is not the modelling technique itself; rather it is dealing with the uncertainties in a sensible manner. Many simplified design orientated approaches are available to analyse the seismic response of pile foundations (Cubrinovski and Ishihara 2004; Cubrinovski and Ishihara 2006; Cubrinovski *et al.* 2006a; Liyanapathirana and Poulos 2005; O'Rourke *et al.* 1994; Tokimatsu *et al.* 2005; Wang and Reese 1998).

In this paper a pseudo-static analysis procedure proposed in Cubrinovski *et al.* (2006a) is examined, somewhat in detail. This analysis uses a beam spring model and can be performed using common site investigation data such as the SPT blow count, yet it captures the basic mechanism of pile behaviour. Presented here are details of the adopted modelling technique and its application to a case study of a bridge foundation in liquefiable soil. The key input parameters of the model, namely the magnitude of applied free field ground displacement, the degradation of soil stiffness and strength due to liquefaction and the magnitude of inertial load from the superstructure are varied parametrically to identify important features of the response. The objectives of the paper are to determine how variations in these key parameters affect the soil-pile interaction and to emphasise the need to consider a wide range of values of input parameters when simplified analysis is performed.

BEAM-SPRING MODEL

Analytical Model

The analytical model used in this paper is based on a simplified three layer model described in Cubrinovski and Ishihara (2004) that consists of a non liquefiable crust layer, liquefied layers and a non-liquefied base layer. The original model used a closed form solution to solve a three layer problem; here a more rigorous model was adopted where a finite element (FE) beam-spring model is used to incorporate more complex soil layering. Figure 1 shows the analytical model: the pile is modelled as a beam connected to a series of springs representing the lateral stiffness of the soil. The effects of liquefaction on the soil are accounted for by degrading the stiffness of the soil springs and limiting the lateral force in the liquefied layers.

[1] *Geotechnical Engineer, Tonkin and Taylor Ltd., Christchurch (Member).*

[2] *Associate Professor, Department of Civil Engineering, University of Canterbury, Christchurch (Member).*

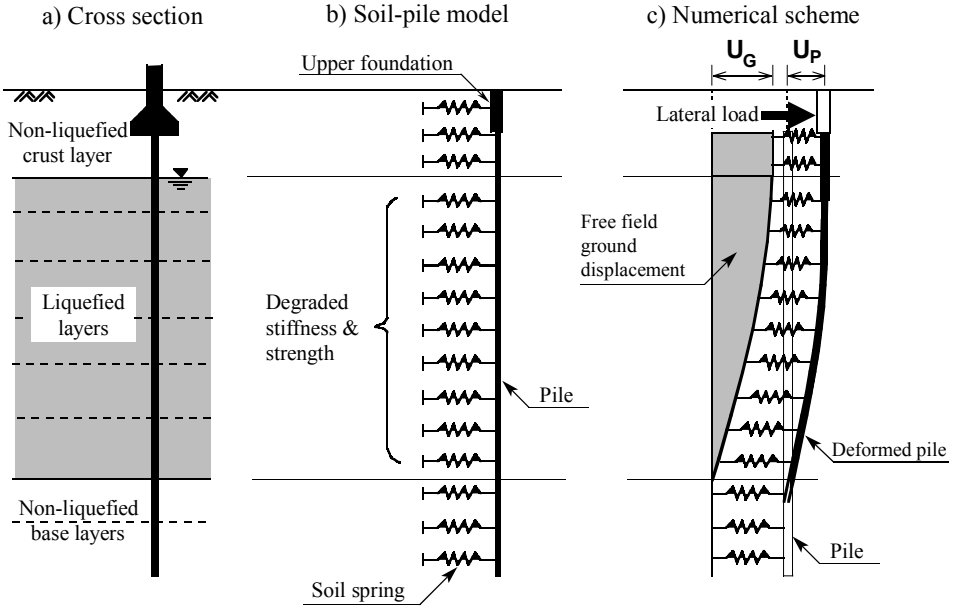

Figure 1. Adopted model for simplified pseudo-static analysis.

The complex dynamic forces applied to piles in liquefied soil are approximated by the sum of two static loads applied to the pile:

(1) Kinematic loads from the soil movement are applied through free field ground displacements acting on a series of soil springs, as shown in Figure 1. These displacements can represent either cyclic ground displacements or lateral spreading displacements of liquefied soils. Note that these are free field ground displacements unaffected by the presence or response of the pile foundation.

(2) Inertial loads from the superstructure are modelled as a lateral point load applied at the pile head. It was adopted in the analysis that this load acts in the same direction as the applied ground displacement.

In the pseudo-static analyses, the cyclic phase of the loading and subsequent lateral spreading phase were considered separately since the loads and soil conditions (stiffness and strength) are greatly different between these two phases.

Input Parameters

The input parameters of the model are summarized in Figure 2 for a three layer model configuration. Soil springs are represented using bi-linear *p-δ* relationships, with an initial stiffness *k* and ultimate pressure p_{max}. Here δ represents the relative displacement between the pile and the soil. In liquefied soil layers the loss of stiffness is represented by a degradation factor, β. The pile is modelled as a beam with diameter D_o and a tri-linear moment-curvature (M-ϕ) relationship. The three points on the M-ϕ curve correspond to the cracking, yielding and ultimate moments of the pile. The FE model allows complex soil layering to be taken into account; changes in soil stiffness between layers and different pile diameters throughout the depth can be incorporated easily into the model.

The external loads on the pile are modelled using a lateral ground displacement U_G and an inertial load F. The ground displacement applied to the pile can take any form throughout the soil profile; U_G represents the maximum lateral ground displacement at the top of the liquefied soil layer and also represents the movement of the crust layer in the free field.

Key Parameters and Uncertainties

Cubrinovski and Ishihara (2004) identified the following key parameters affecting the pile response:

- The stiffness and strength of the liquefied soils, β and $p_{2\text{-}max}$
- The ultimate pressure exerted by the crust layer, $p_{1\text{-}max}$
- The magnitude of the lateral ground displacement, U_G
- The inertial load applied, F

The intrinsic uncertainties associated with piles in liquefiable ground are directly reflected on these key parameters. Therefore for the analysis of piles in liquefiable soil these parameters should not be uniquely determined; rather a range of values should be considered. For this reason a parametric study was performed on a case study to examine how variations in these four key parameters affect the pile response.

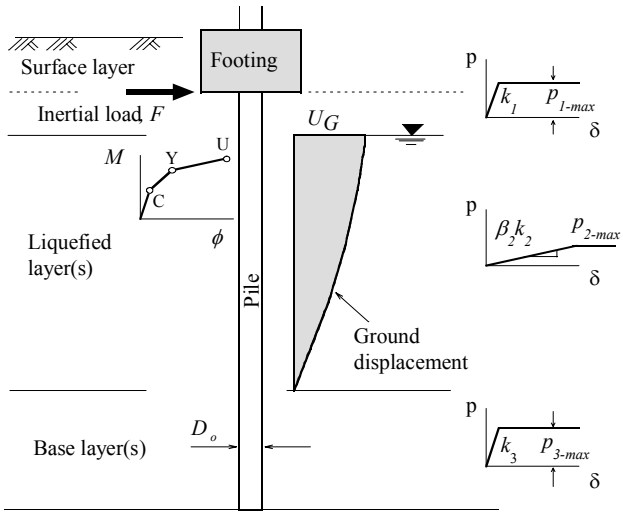

Figure 2. Input parameters and characterisation of non-linear behaviour for pseudo-static analysis.

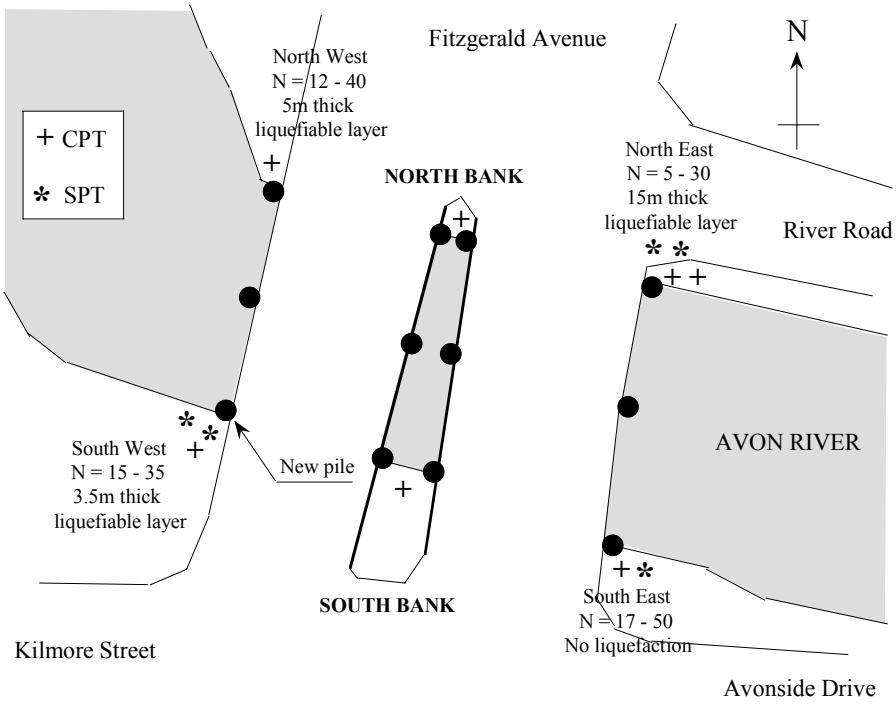

Figure 3. Plan view of the bridge site, showing site investigation locations and summary of penetration resistance results.

CASE STUDY

To illustrate the effects of variation in key parameters on the pile performance, parametric studies were conducted on a case study of twin bridges crossing the Avon River in Christchurch, New Zealand. The Fitzgerald Avenue Twin Bridges cross the Avon River, carrying three lanes of southbound traffic on the east bridge and two lanes of northbound traffic on the west bridge. Both bridges are supported by piled abutments on the banks with a central piled pier at the mid-span. According to the initial investigations, the existing piles were founded on potentially liquefiable soils.

The bridges have been identified as an important lifeline for post-disaster emergency services and recovery operations. To avoid structural failure of the foundations or significant damage causing loss of function of the bridge in an anticipated earthquake event, a structural retrofit has been proposed by the Christchurch City Council. In conjunction with bridge widening, this retrofit involves strengthening of the foundation with new large diameter bored piles to be installed; the location of the new piles are shown schematically by the solid circles in Figure 3. The new piles will be connected rigidly to the existing foundation and superstructure, and founded into deeper strata consisting of non-liquefiable soils.

Soil Conditions

Detailed investigations were conducted at several locations at the site using SPT and CPT, as indicated in Figure 3. The results of these field tests reveal the highly variable stratigraphy and penetration resistance of the investigated locations. Testing was conducted on the north and south banks of the river, at locations on both the east and west sides of the bridge and in between the two bridges. The site investigation data is summarised in Figure 3, showing the inferred range of SPT blow counts at the four corners of the bridge.

The occurrence of liquefaction at the site was assessed based on the results of the *in situ* testing and by considering the ground shaking hazard. In general the soil on the north bank is looser and more susceptible to liquefaction than the soil on the south bank.

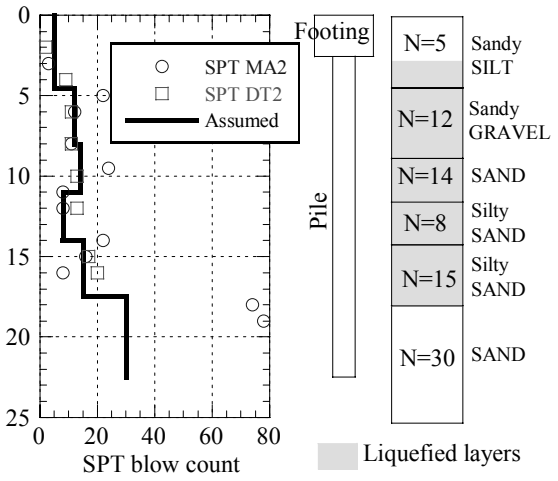

Figure 4. Soil profile, CPT and SPT results for the north–east corner.

This is consistent with the assumed nature of soil deposition at the site; the north bank is on the inside of a bend in the river while the south bank is on the outside. As the river has progressed soil has been eroded from the outside of bends and deposited on the insides, thus the soil on the inside of a bend is likely to have been laterally accreted in a low energy environment.

The worst soil conditions were encountered at the North-East corner; the analysis in this paper is based on the soil properties at this corner and hence represents a conservative assessment. Here the soil between 2.5 m and 17.5 m is considered to be liquefiable, with layers of silty sand, sandy gravel, sandy silt and sand, with a dense sand base layer below 17.5 m depth. Figure 4 shows the results of SPT and CPT testing; the assumed soil profile and SPT blow counts used in the analysis are also shown. From the CPT results at the north east corner, a fines content of approximately 10% was inferred for the liquefiable soil.

BRIDGE FOUNDATION

Figure 5 shows a cross section of the east bridge; the abutments and piers are supported by driven reinforced concrete piles connected to a reinforced concrete pile-cap at the river level. The existing piles are approximately 10-11 m in length and 0.3 m in diameter. The central pier is supported by 8 existing piles at 5*D* spacing; the abutments are supported by four vertical piles and five raked piles at 4*D* spacing. The two bridges have identical foundations and the river level is approximately 2.5 m below the road level.

The proposed new piles will be founded at a depth below the expected depth of liquefaction and installed outside the existing pile cap. In conjunction with proposed widening of the bridge the pile cap will be extended and the new piles will be rigidly connected to the superstructure. The new piles will be steel-encased reinforced concrete piles designed to carry the entire load from the existing bridge and any additional loads from the bridge widening. Shown in Figure 5 are the proposed piles; they are 1.2 m in diameter under the abutments and 1.5 m in diameter under the central pier.

Seismic Hazard

Previous seismic hazard studies for Christchurch (Dowrick *et al*. 1998; Stirling *et al.* 2001) indicate that the most significant contribution to the ground shaking hazard arises from a magnitude 7.2-7.4 event on the strike-slip Porters Pass fault, which is located at a distance of about 40-60 km from the site. Stirling *et al*. (2001) give the following peak ground acceleration values for Christchurch:

- 0.25g in a 150 year event
- 0.37g in a 475 year event and
- 0.47g in a 1000 year event.

With regard to the importance level of the bridge as a lifeline, the loadings standard NZS1170.5 requires an ultimate limit state (ULS) design seismic event with an annual probability of exceedance of 1/2500, i.e. a 2500 year event. This corresponds to a peak ground acceleration of 0.44g, as calculated in NZS1170.5 based on the soil conditions and period of the structure. This is roughly in agreement with the above mentioned peak ground acceleration from Stirling *et al.* (2001).

Determination of Material Parameters

As the procedure is a simplified, design orientated approach, all input parameters can be determined using empirical correlations with common site investigation data. The input parameters can be divided into the four categories; soil properties (k, p_{max}), effects of liquefaction on the soil stiffness and strength (β, S_u), pile properties (D_0, M-ϕ curve) and external loads (U_G and F).

Soil properties

The stiffness and ultimate pressure of the soil springs were evaluated using correlations with the SPT blow count, N. The stiffness was calculated by first evaluating the subgrade reaction coefficient, κ, using an empirical formula (Architectural Institute of Japan 2001):

$$\kappa = 56\,(N_{78})\,D_o^{-3/4} \quad [\mathrm{MN/m^3}] \tag{1}$$

where N_{78} is the SPT blow count corresponding to 78% of the theoretical free fall energy and D_o is the pile diameter in cm. The stiffness, k, is then evaluated by the formula

$$k = \kappa\, D_0\, l \tag{2}$$

where l is the spacing between nodes or the length of the beam element used in the FE analytical model. The ultimate pressure, p_{max}, exerted by the soil on the pile in non-liquefied soil is given by the expression

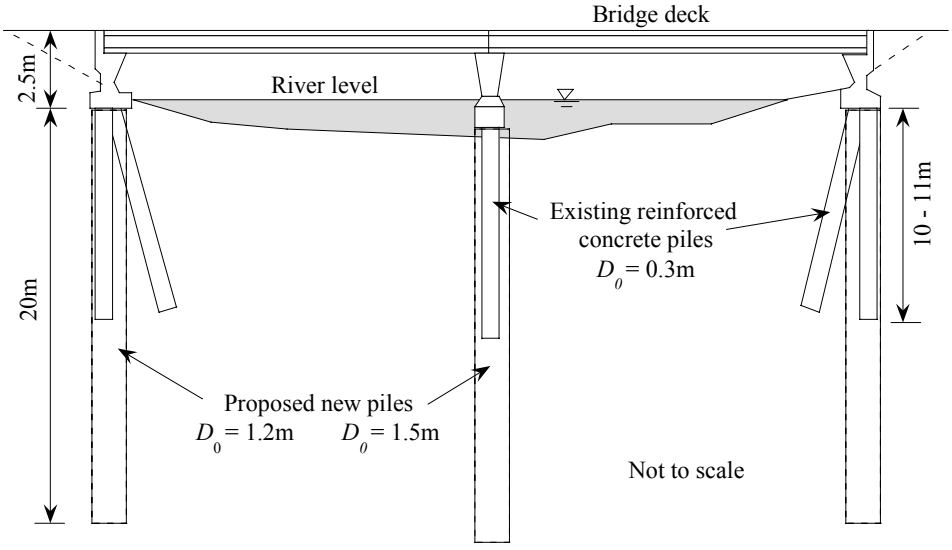

Figure 5. Bridge cross section showing existing piles and proposed new piles.

$$p_{max} = \alpha_u \, p_p(z) \quad (3)$$

where $p_p(z)$ is the Rankine passive pressure as a function of depth and α_u is a factor introduced to account for the difference in lateral pressure between a single pile and an equivalent wall. Note that α_u may take a value as high as 4.5 in the non-liquefied crust. The Rankine passive pressure is calculated as

$$p_p(z) = K_p \sigma'_v \quad (4)$$

where σ'_v is the vertical effective stress and K_p is Rankine passive earth pressure coefficient calculated as (Hatanka and Uchida, 1996)

$$K_p = \tan^2(45 + \phi/2) \quad (5)$$

where ϕ can be estimated, for example as

$$\phi = 20 + (20 N_{1(78)})^{0.5} \quad (6)$$

The SPT blow count normalised to an effective overburden stress of 98 kPa (N_1) can be calculated using the expression of Liao and Whitman (1986)

$$N_1 = N\left(\frac{98}{\sigma_v'}\right)^{0.5} \quad (7)$$

Note that the SPT blow count corresponding to 78% energy of the theoretical free fall energy is given by

$$N_{78} = \frac{60}{78} N_{60} \quad (8)$$

Here $N_{1(60)}$ is an SPT blow count normalised for the effective overburden stress corresponding to 60% energy of the theoretical free fall energy, where $N_{(60)}$ is an SPT blow count corresponding to 60% of the theoretical free fall energy.

Effects of liquefaction on soil stiffness and strength

In liquefied soil the stiffness k is degraded by a factor β which is less than one. With reference to case studies and experimental tests (Cubrinovski *et al.* 2006b; Ishihara and Cubrinovski 1998; O'Rourke *et al.* 1994; Orense *et al.* 2000; Tokimatsu *et al.* 2005; Yasuda and Berrill 2000), the stiffness degradation of liquefied soils can be assumed to vary between β = 1/10 and 1/50 for the cyclic phase cases, and between β = 1/50 and 1/1000 for lateral spreading cases. The prediction of the liquefied soil stiffness is very difficult and depends on many factors, including the density of the soil, development of excess pore pressures, the magnitude and rate of ground displacement and the drainage conditions. Furthermore, full scale shake table tests (Cubrinovski *et al.* 2006b) show that the stiffness of liquefied soils varies considerably during the course of both the cyclic and lateral spreading phases.

The ultimate pressure exerted on the piles from the liquefied soil is also subject to uncertainty. The interaction in the liquefied layer can be treated in a simplified manner by an equivalent linear p-δ relationship with a degraded stiffness and no limiting ultimate pressure. Alternatively and more rigorously, a limit can be placed on the pressure exerted by the liquefied soil. The approach used herein is to define the ultimate pressure from the liquefied layers, $p_{2\text{-}max}$, using the undrained or residual strength of the sandy soils, S_u. Here S_u is evaluated from empirical correlation with SPT value originally proposed by Seed and Harder (1990) as shown in Figure 6. The data in this figure were back calculated from case history observations during previous earthquakes in which flow slides occurred. Post-earthquake static stability analyses were conducted by many researchers (Idriss and Boulanger 2007; Olson and Stark 2002; Seed 1987; Seed and Harder 1990) investigating liquefaction flow slides; the undrained shear strength was estimated by back calculating a value of S_u based on the deformed geometry after the event. Hence in this plot, each point represents the estimate of S_u for one case history. Since the scatter of the data is quite significant, an upper ($S_{u\text{-}ub}$) and lower bound ($S_{u\text{-}lb}$) values as indicted in Figure 8 were used to cover the range of values.

Table 1 summarises the soil properties used in the analysis of cyclic and lateral spreading cases, as calculated according to the expressions and procedures outlined above.

Pile properties

The yielding, cracking and ultimate points of the pile were calculated by assuming that the concrete and reinforcing steel are elastic-perfectly plastic materials with bi-linear stress strain relationships. By specifying the pile cross section and characteristics (dimensions, area and position of reinforcement, Young's modulus and strengths of materials, prestress level, axial force) the tri-linear moment curvature relationship of the pile was calculated. The three points are defined as follows:

Table 1. Soil properties used in parametric study

	Description	Stiffness, k (kN/m)				Ultimate pressure, $p_{2\text{-}max}$ (kPa)	
		Cyclic phase		Lateral spreading		$S_{u\text{-}lb}$	$S_{u\text{-}ub}$
		β_{lb}=1/10	β_{ub} =1/50	β_{lb} =1/50	β_{ub} =1/1000		
1	Crust layer	1853				K_p = 3.6	
2	Sandy SILT	185	37.1	37.1	1.85	2	28
3	Sandy GRAVEL	445	89.0	89.0	4.45	17	43
4	SAND	519	104.8	104.8	5.19	17	43
5	Silty SAND	297	59.3	59.3	2.97	2	28
6	Silty SAND	556	111.2	111.2	5.56	10	33
7	SAND	11121				410	

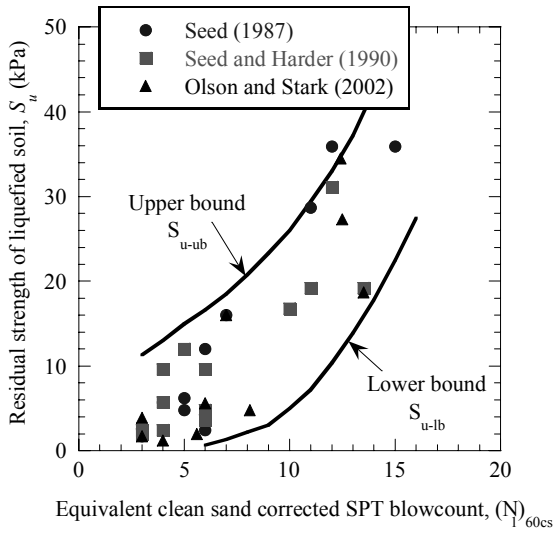

Figure 6. Empirical chart used to evaluate ultimate pressure exerted by liquefied soil through undrained shear strength (after Idriss and Boulanger 2007).

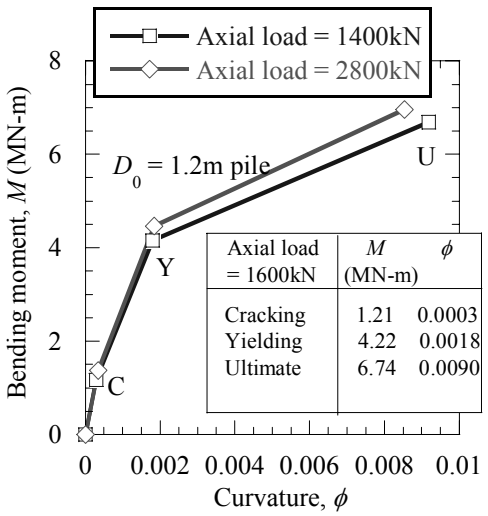

Figure 7. Moment curvature relationship for the new 1.2 m pile.

(1) Cracking is the point where the tensile stress in the concrete exceeds the concrete tensile strength.

(2) Yielding is the point where the stress in the reinforcement exceeds the yield level.

(3) Ultimate is the point where compressive strain in the concrete exceeds the ultimate concrete compressive strain level, usually in the range between 0.0025 and 0.0035.

The moment curvature relationship for the new 1.2m diameter pile was calculated assuming 30 MPa concrete, 500 MPa steel reinforcement at a 0.8% longitudinal reinforcement ratio and a 10 mm thick steel casing with a strength of 250 MPa. The axial loads on the piles are preliminary estimates; Figure 7 shows the calculated M-ϕ relationships for both the serviceability limit state (SLS) and the ultimate limit state (ULS) axial loads to give an indication of the effect of increasing axial load on the pile bending capacity. For consideration of the seismic response an axial load of 1600 kN was used. This axial load is a preliminary estimate only, based on the likely bridge weight and traffic loading.

External loads

Two external loads are applied to the pile: an inertial force at the pile head and a ground displacement. The level of inertial load applied at the pile head can be calculated as the ground acceleration times the tributary mass of the superstructure taken by the pile. The level of acceleration can either be the peak ground acceleration or a lesser value. For the pile at the north east corner, the maximum inertial load considered was calculated as the tributary superstructure mass of 1600 kN multiplied by the peak ground acceleration of 0.44g giving a maximum inertial load of 704 kN.

In the analysis the lateral ground displacement can represent either cyclic displacements during the shaking phase or a permanent displacement at the end of the spreading phase. Lateral spreading displacements were modelled as having a cosine distribution throughout the liquefied layers, with a displacement at the ground surface, U_G, describing the magnitude of the ground movement. Many empirical methods exist for predicting this displacement (e.g. Ishihara *et al.* 1997; Tokimatsu and Asaka 1998; Youd *et al.* 2002) however it is very difficult to make an accurate prediction.

The magnitude of lateral spreading at the north east corner was predicted using the method of Youd *et al.* (2002). A free face height of 2.5 m was assumed, and a displacement of 2.2 m was calculated at the riverbank. Due to the considerable uncertainty in predicting the ground displacement Youd *et al.* suggest a factor of 2 be used for displacements predicted using their model to cover the range of expected values. With this in mind, and considering the large differences between different empirical methods, a wide range of values were considered in the parametric study.

Maximum cyclic ground displacements in liquefied soils during the cyclic phase were estimated using a simplified procedure described in Tokimatsu and Asaka (1998). The procedure is based on observations from previous earthquakes, where cyclic shear strains in liquefied soil layers were evaluated from analysis of strong motion records and detailed surveys of piles in level ground and then plotted against SPT value, as shown in Figure 8. The chart is essentially equivalent to the conventional SPT-based charts for evaluation of liquefaction; the cyclic stress ratio τ_{av}/σ'_{vo} on the y-axis is calculated using the standard method of Seed and Idriss (Youd *et al.* 2001).

To estimate the cyclic ground displacement, for each liquefied soil layer the cyclic shear strain is first evaluated using the chart. Then, these strains are integrated throughout the soil profile to obtain a cyclic ground displacement profile. Shown in Figure 8 is the calculation of the induced cyclic shear strain for a soil layer with a corrected SPT blow count for clean sand of $N_{1(60)cs}$=14 and a cyclic stress ratio of τ_{av}/σ'_{vo} = 0.43. Note that the SPT blow count in Figure 8 implicitly corresponds to 78% of the theoretical free fall energy, even though data from 60-78% have been used in the derivation of the plot. In view of the differences in the correction of the blow count for the effects of fines and highly approximate nature of the plot, it is considered appropriate to use this plot without correcting the blow count with the energy ratio. For the North-East corner soil profile, Figure 9 shows the maximum shear strains and corresponding maximum cyclic horizontal ground displacements calculated using the procedure described above.

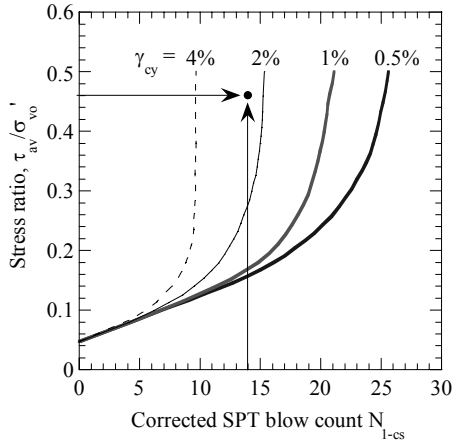

Figure 8. Empirical chart used to evaluate cyclic ground displacements through induced shear strains (after Tokimatsu and Asaka 1998). Shown is the shear strain evaluated for a soil layer with $(N_1)_{60cs}$ =14 and τ_{av}/σ'_{vo} = 0.43.

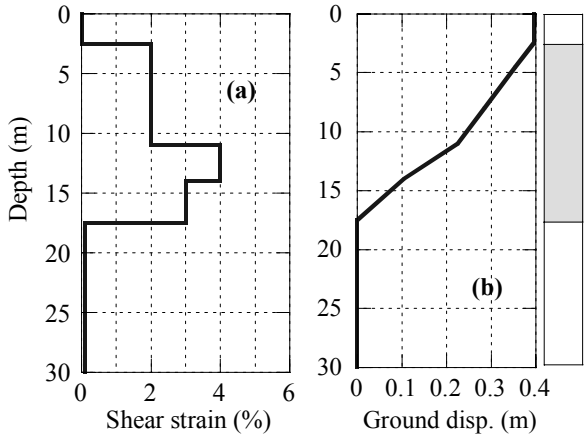

Figure 9. Liquefaction induced cyclic ground deformation: (a) maximum cyclic shear strains, (b) maximum cyclic ground displacement profile.

PARAMETRIC STUDY

Overview

The seismic response of the proposed 1.2 m diameter pile at the north-east corner is evaluated using the pseudo static approach described previously. The identified key parameters are varied to account for uncertainties in the analysis; this is to gain insight into how variations in these parameters affect the analysis results. In all analyses the properties of the pile, the crust and base soil layers were kept constant.

The two phases in the response, the cyclic phase and lateral spreading, were treated separately. In cyclic phase analyses, an inertial load was applied at the pile head in addition to the ground displacement shown in Figure 9b. In contrast, the lateral spreading cases have no inertial load and the ground displacement has a cosine profile throughout the liquefied layers with a magnitude U_G at the top of the liquefied layer. Lateral spreading cases with reduced inertial loads were also considered but are not discussed herein. Note that a potential damage to the pile caused during the cyclic phase was not considered in the analysis of the subsequent lateral spreading phase. In other words, in this simplified interpretation, intact properties of the pile were used in the lateral spreading analysis.

Typical Results

In order to demonstrate key features of the pile response, one analysis case is described in detail. Figure 10 shows the results of a lateral spreading analysis, where the magnitude of free field ground displacement was one metre, and relatively high degradation of stiffness and strength was used with β = 1/1000 and $p_{2\text{-}max} = S_{u\text{-}lb}$ (which corresponds to a range of 2-17kPa throughout the liquefied layers).

Figure 10a shows the computed bending moment distribution with reference to the cracking, yielding and ultimate moments of the pile. It can be seen that the maximum moments occur at the pile head and at the interface between the liquefied and base layers, and that the bending moment exceeds the yield level at the pile head. Figure 10b shows the pile displacement compared to the free field ground displacement. The pile exhibits behaviour typical of stiff piles, and resists the large lateral movement of the surrounding soils. The resulting relative displacement between the soil and the pile is therefore quite large as shown in Figure 10c.

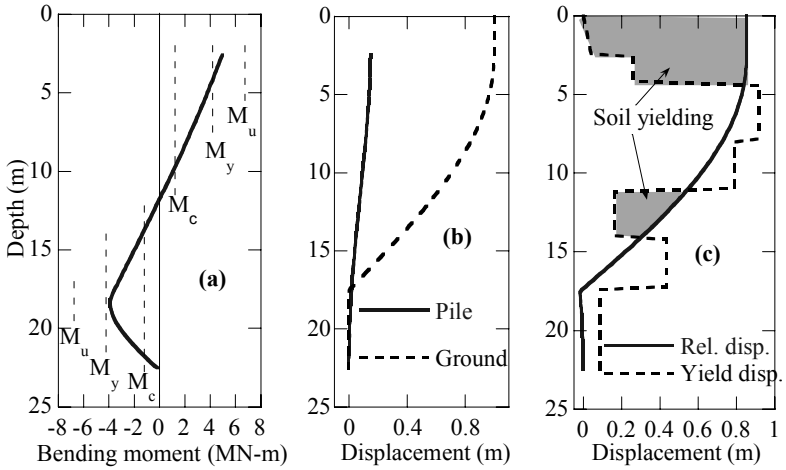

Figure 10. Results of typical analysis showing the pile response to a lateral spreading displacement of one metre: (a) bending moment versus depth plot; (b) pile and ground displacements; and (c) relative displacement between the soil and pile compared to the soil yield displacement.

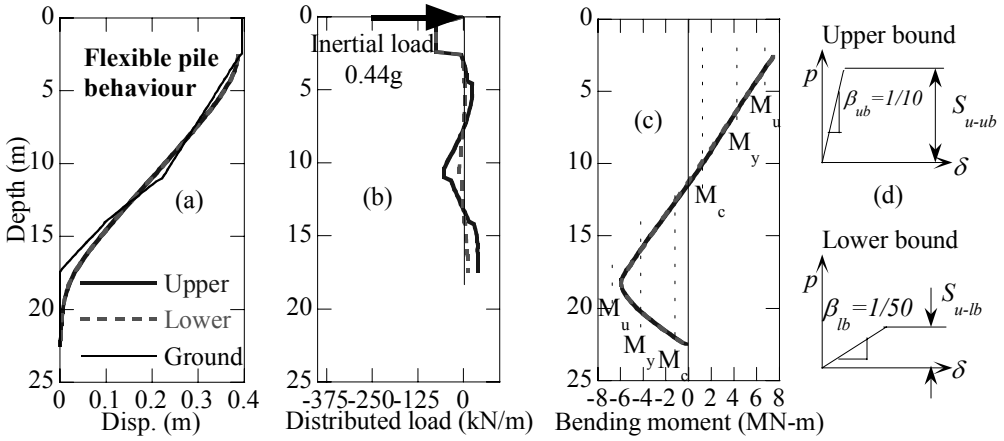

Figure 11. ***Variation of pile response due to liquefied layer properties for a cyclic phase case with a large inertial load, showing pile displacement, distributed load on the pile and pile bending moment.***

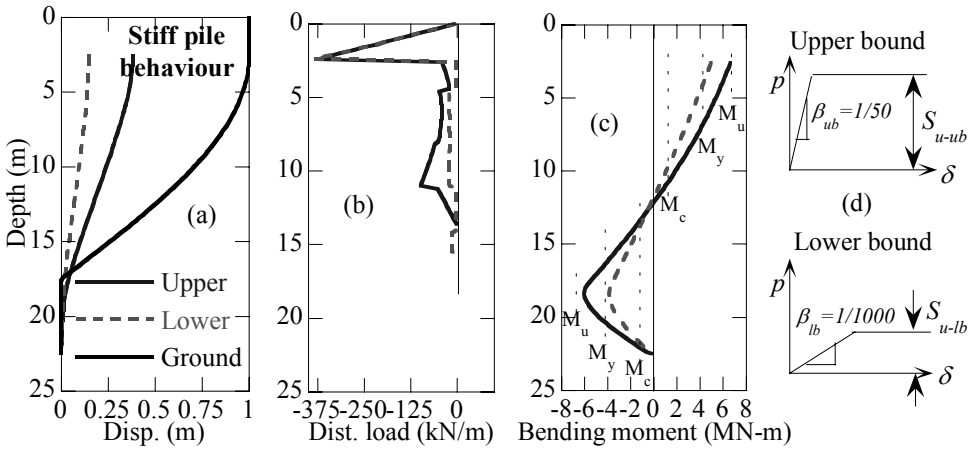

Figure 12. ***Variation of pile response due to liquefied layer properties for a lateral spreading case with U_G = 1 m, showing pile displacement, distributed load on the pile and pile bending moment.***

The dashed line in this figure indicates the relative displacement δ_y at which yielding occurs in the soil or the displacement at which $p_{2\text{-}max}$ has been reached in the bi-linear relationship. Hence the shaded areas indicate parts of the soil profile where the relative displacement exceeds the yield level of the soil; here the pressure acting on the pile has reached the maximum level as defined by the p-δ relationship.

Degradation of Liquefied Soil Stiffness and Strength

Due to the uncertainty of the effect of liquefaction on the soil stiffness and strength, analyses were conducted using two p-δ relationships, an upper bound and lower bound p-δ curve. In this way two extremes of liquefied soil stiffness and strength were considered, with the upper bound p-δ curve combining, for lateral spreading cases, a stiffness degradation of β = 1/50 and $p_{2\text{-}max} = S_{u\text{-}ub}$. Conversely, the lower bound p-δ curve was defined by β = 1/1000 and $p_{2\text{-}max} = S_{u\text{-}lb}$. For the cyclic cases the upper bound p-δ curve was defined using β = 1/10 and $p_{2\text{-}max} = S_{u\text{-}ub}$; the cyclic lower bound p-δ curve used β = 1/50 and $p_{2\text{-}max} = S_{u\text{-}lb}$.

Effects on stiff and flexible piles

For both cyclic and lateral spreading phases the pile behaviour depends on the stiffness of the pile relative to the liquefied or displacing soil. Relatively flexible piles move together with the lateral ground displacement; whereas relatively stiff piles resist the movement of the surrounding ground. Therefore to evaluate the effects of different liquefied soil properties on the pile response two cases need to be analysed corresponding to the stiff and flexible behaviour respectively. Needless to say, the stiff pile behaviour is more relevant to design, because the flexible pile behaviour often provides unacceptable performance due to the excessive lateral displacements of the pile and hence the superstructure.

Figure 11 shows the pile response for a cyclic phase analysis where a large inertial load corresponding to 0.44g was applied at the pile head in addition to the maximum cyclic ground displacement shown in Figure 9b. Two cases are shown corresponding to the upper bound and lower bound bi-linear p-δ curves, shown in Figure 11d. Figure 11a shows that for both cases of degradation the pile acts in a flexible manner with little relative displacement between the pile and the soil. It can be seen that despite differences in the forces acting on the pile from the liquefied layers the bending moments and pile displacements are very similar. This suggests that for this flexible pile behaviour the liquefied layer does not have a large bearing on the pile response as the pile behaviour is governed by the large inertial load. Note that due to the small relative displacement between the soil and the pile, the full passive pressure of the crust layer has not been mobilised in this case.

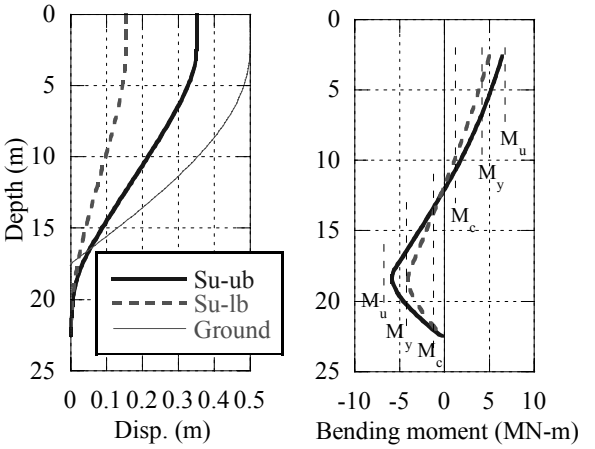

Figure 13. Pile response for a lateral spreading case with U_G = 0.5m and β = 1/50, showing the effects of ultimate pressure from the liquefied soil.

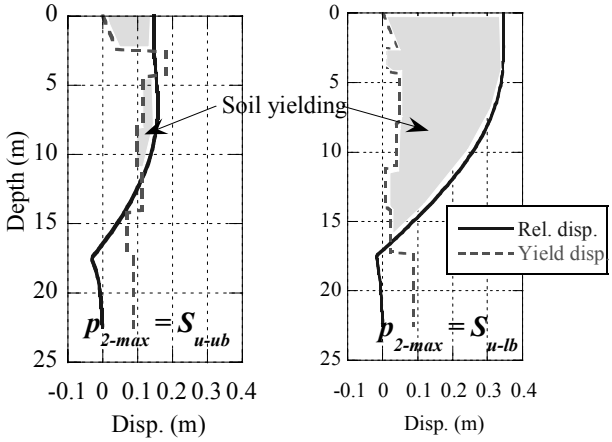

Figure 14. Comparison of relative and yield displacements computed in analyses with $p_{2\text{-}max} = S_{u\text{-}lb}$ and $p_{2\text{-}max} = S_{u\text{-}ub}$

In contrast, Figure 12 shows the results of a lateral spreading analysis with different liquefied soil properties and no inertial load. Here, both cases of upper bound and lower bound p-δ curves show stiff pile behaviour, as such the large relative displacements between the pile and the soil result in the liquefied soil properties having a significant effect on the pile response. For the upper bound liquefied p-δ relationship the forces from the liquefied soil are larger, resulting in larger pile displacements and bending moments than those observed for the lower bound p-δ curve. Because of the large relative displacements, in both cases stiff pile behaviour was observed, resulting in full mobilisation of the passive load from the non-liquefied crust soil. In the absence of a large inertial load, the pile exhibited stiffer behaviour and the loads from the crust and liquefied layers had a larger effect on the pile response.

Effect of ultimate pressure, $p_{2\text{-}max}$

To examine how the ultimate pressure exerted by the liquefied soil on the pile affects the pile response, two analyses were conducted on a lateral spreading case with U_G = 0.5 m and β at 1/50. Figure 13 shows the computed pile response for cases where (a) the ultimate pressure was limited to $p_{2\text{-}max} = S_{u\text{-}lb}$ (in the range of 2 – 17 kPa), and (b) $p_{2\text{-}max} = S_{u\text{-}ub}$ (28 – 43 kPa). It can be seen that adopting $p_{2\text{-}max} = S_{u\text{-}ub}$ for the ultimate pressure in the liquefied soil results in more flexible behaviour and higher bending moments than the $p_{2\text{-}max} = S_{u\text{-}lb}$ case. These observations can be explained by considering the relative displacements between the soil and the pile for both cases.

Figure 14 shows the relative displacement between the soil and the pile plotted with the soil yield displacement for the two cases. It can be seen that the lower bound S_u case has low yield displacements and high relative displacements, whereas the upper bound S_u case has higher yield displacements and lower relative displacements. A large part of the soil profile has yielded with the lower bound case of $p_{2\text{-}max} = S_{u\text{-}lb}$, thus the pressure is limited to $S_{u\text{-}lb}$ for a large length of the pile in this case.

Forces from the crust soil and liquefied soil

In the case of stiff pile behaviour, the soil pressure from the crust and liquefied layers provide a driving force, while the non-liquefied base layer provides a resisting force. With changes in the liquefied soil stiffness and strength the forces applied to the pile from both the crust and liquefied layers change. To quantify these changes lateral spreading analyses were conducted using U_G = 0.5 m with the ultimate pressure in the liquefied layer given by $p_{2\text{-}max} = S_{u\text{-}ub}$ or $p_{2\text{-}max} = S_{u\text{-}lb}$. In both cases the stiffness degradation β varied from 1/50 to 1/1000 and the total force on the pile, including contributions from the crust and liquefied layers, was calculated and plotted against β as shown in Figure 15.

It was observed that all cases exhibited stiff pile behaviour; the piles in general resisted the ground movement and the bending moments exceeded the yield level at the pile head. It was observed that the total load from the crust layer remained the same regardless of β or S_u. This is because the large relative displacements between the stiff pile and the soil caused the entire crust layer to yield. For the $p_{2\text{-}max} = S_{u\text{-}ub}$ case shown in Figure 15a the load from the liquefied layer increases with increasing β, when β = 1/50 (0.02) the load from the liquefied layer is as large as the load from the crust layer. Figure 15b shows the case where $p_{2\text{-}max} = S_{u\text{-}lb}$ was used; here the load from the liquefied layer is limited by the lower bound ultimate pressure from the liquefied soil.

The same analysis was repeated for a pile with a diameter of 0.6 m to examine the interaction between the crust and liquefied layer loads for more flexible piles. For all these cases flexible behaviour was observed and the pile moved together with the ground; the bending moment reached the ultimate level at the pile head. Figure 16 shows the contribution of loads for the flexible pile cases. Here the load from the crust layer is much smaller than that for the stiff pile cases, and decreases with increasing β. This is because a large β value results in smaller relative displacement between the pile and the soil and hence a lower load from the crust layer. The load from the liquefied layer increases with increasing β, and the combined loads from the crust and liquefied soil result in an increase in the total load as β increases.

Effect of horizontal ground displacement

For stiff piles undergoing lateral spreading, it is interesting to determine how the magnitude of horizontal ground displacement applied, U_G, affects the pile response. As the prediction of lateral spreading displacement is very difficult, and considering the variation in empirical prediction methods, the approach taken here is to consider a wide range of lateral spreading displacements. Figure 17 shows the computed maximum pile displacements for cases with β = *1/50* and U_G = 0.5, 1, 2 and 3 m.

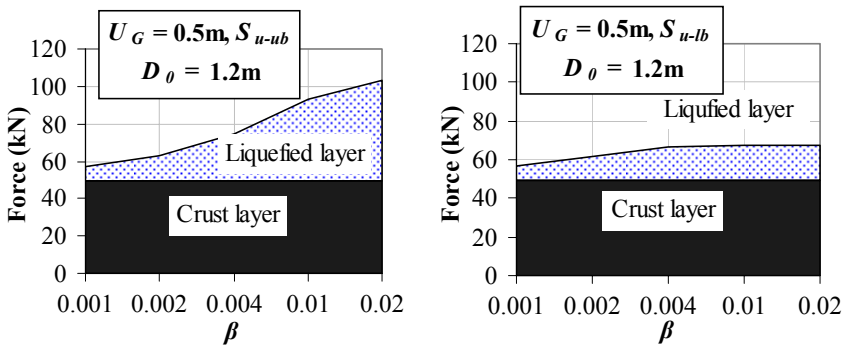

Figure 15. ***Force applied to stiff piles from the crust and liquefied layers as a function of the stiffness degradation due to liquefaction, β.***

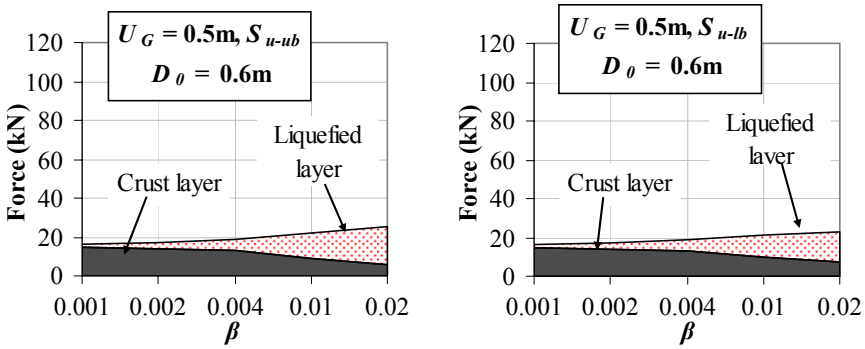

Figure 16. ***Force applied to flexible piles from the crust and liquefied layers as a function of the stiffness degradation due to liquefaction, β.***

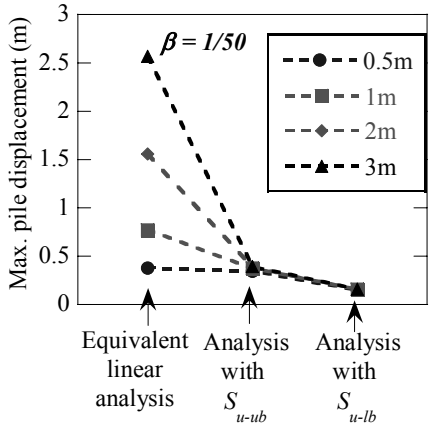

Figure 17. ***Variation of maximum pile displacements with applied lateral ground displacement for different values of ultimate pressure from the liquefied soil.***

Results are calculated using three different p-δ curves for the liquefied soil; one without ultimate pressure in the liquefied soil (equivalent linear case), while the other two cases use $p_{2\text{-}max} = S_{u\text{-}ub}$ and $p_{2\text{-}max} = S_{u\text{-}lb}$ to limit the ultimate pressure. For the equivalent linear case the pile displacement increases with increasing ground displacement and the pile exhibits flexible behaviour. The equivalent linear cases predicted flexible behaviour and very large values of pile bending moment; at U_G = 3 m the bending moment is well in excess of the ultimate moment of the pile. This result is unrealistic because the ultimate load from the liquefied soil exceeded any reasonable limit. Therefore the more rigorous p-δ curves with a limit on the ultimate pressure are necessary for cases with large relative displacements between the soil and the pile. In contrast, when limits are placed on the ultimate pressure in the liquefied soil, stiff pile behaviour is observed, and the magnitude of ground displacement has virtually no effect on the pile response. This observation is hardly surprising given that in these cases the applied ground displacement is sufficient to cause the vast majority of the soil profile to yield, thus for these cases the same lateral load corresponding to the limiting pressure is being exerted on the pile.

The above behaviour suggests that for a given pile a critical magnitude of U_G exists above which any increase in lateral ground displacement will have no effect on the pile response. In order to scrutinise this, a series of analyses were conducted with different values of applied ground displacement U_G using different values of β and $p_{2\text{-}max}$.The results of these analyses are shown in Figure 18, which plots the calculated pile displacement against the value of U_G applied in the analysis. Figure 18 shows that this threshold ground displacement exists; as the applied lateral ground displacement is increased a certain level is reached above which any further increase in the displacement has no effect on the pile response. It is also apparent that this critical value depends on the stiffness degradation constant β and the ultimate pressure $p_{2\text{-}max}$. Figure 19 plots this threshold value against β, where $U_{G\text{-}threshold}$ is defined as the applied ground displacement that results in a pile displacement which is 95% of the pile displacement calculated using a very large ground displacement. Quantitatively, for the $p_{2\text{-}max} = S_{u\text{-}ub}$ case, this is defined as 0.37m, which corresponds to 95% of 0.39 m, the pile displacement calculated using a U_G value of 5 m. The critical value decreases as β is increased and is $U_{G\text{-}threshold}$ = 0.6 m and 2.3 m for β = 1/50 and 1/500 respectively. It is apparent from Figure 18 that $U_{G\text{-}threshold}$ is much smaller in the $p_{2\text{-}max} = S_{u\text{-}lb}$ cases.

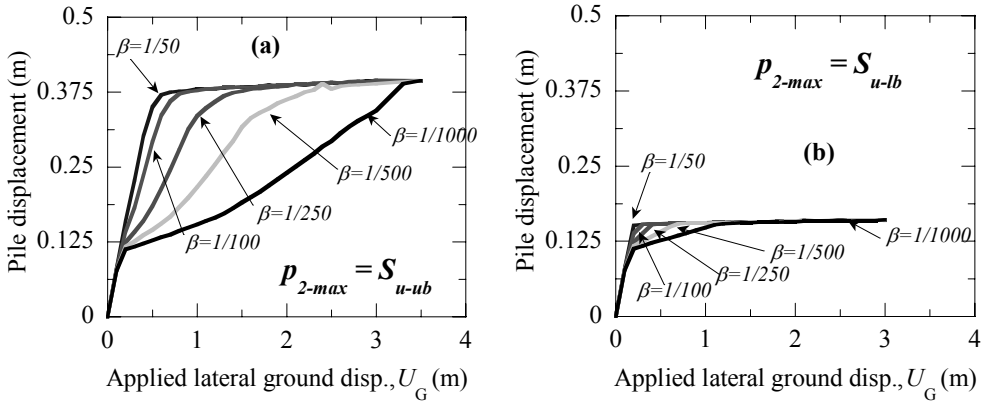

Figure 18. Plot of maximum bending moment versus applied ground displacement for different values of β.

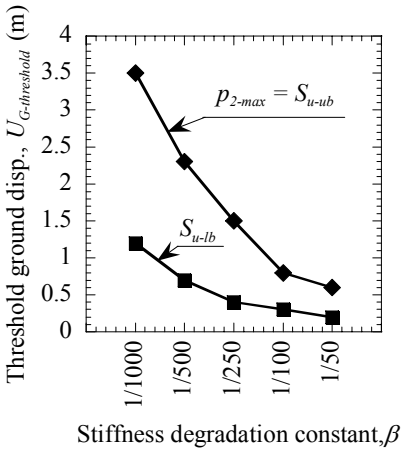

Figure 19. Critical ground displacement above which any further increases in U_G have no effect on the pile response plotted against stiffness degradation in the liquefied soil.

To illustrate the implications of Figure 19, suppose a β value of 1/100 was assumed. Figure 19 indicates that for any value of ground displacement greater than 0.8 practically the same pile response will be obtained when $p_{2\text{-}max} = S_{u\text{-}ub}$ is used. In other words, the accuracy in evaluating U_G is not relevant if the value of 0.8 m could be exceeded.

Effect of loads at the pile head

In the pseudo static analysis procedure two loads are applied at the top of the pile; a point load representing the inertial loads from the superstructure, and a distributed load from the passive pressure exerted by the crust layer on the footing. Both these loads can vary in magnitude. The passive pressure exerted on the pile by the non-liquefied crust is generally only fully mobilised once a certain yield displacement in the soil is reached. Consequently flexible piles with small relative displacements will experience a smaller load when compared with a stiff pile where the full passive pressure has been mobilised in the crust layer.

The level of inertial load applied at the pile head is generally calculated using the peak ground acceleration and tributary mass for the pile. Analysis during the cyclic phase considers the pile response when the ground displacement is at a maximum; however the maximum inertial load is not necessarily being applied at the same time. Large-scale shaking table tests (Tokimatsu *et al.* 2005) and dynamic finite element analyses (Chang *et al.* 2005) have indicated that inertial loads and cyclic ground displacements act in phase when the natural period of the superstructure is less than that of the ground. Nevertheless there is a need to examine how variations in the combination of the inertial and crust loads affect the pile response. The effects of loads at the pile head have a large effect on the pile response; large loads can cause the pile to act in a flexible manner, while stiffer behaviour can be observed with no inertial load applied. Thus, it is interesting to examine the effect that loads applied at the pile head have on the response of piles.

The combination of inertial and crust layer loads can be discussed with reference to the total load applied at the pile head, as both loads act at practically the same location they produce similar effects on the pile response. Cyclic phase analyses with different loads at the pile head were conducted to determine how the addition of these two loads affects the pile behaviour. Six combinations of loads were analysed, corresponding to

- Three cases with inertial loads equivalent to peak ground accelerations of 0.44g, 0.22g and 0g using the original soil profile, and
- Three cases with the same inertial loads as above but using a soil profile without a crust layer.

As before, analyses with upper and lower bounds of p-δ relationships for the liquefied soil were conducted, the loads from the crust layer and the inertial loads for all twelve analysis cases are summarised in Table 2. The maximum load from the crust layer is 490 kN; this is observed in cases where the relative displacement between the soil and the pile is large enough to cause all of the crust layer to yield. Figure 20 shows the results of these analyses, where the peak pile displacements and bending moments were plotted against the total load at the pile head for both upper and lower bounds of liquefied soil stiffness and strength.

Table 2. Combinations of loads applied at the pile head

	Acc (g)	Inertial load (kN)	Crust load (kN)		Total load (kN)	
			Upper bound β=1/10 $S_{u\text{-}ub}$	Lower bound β=1/50 $S_{u\text{-}lb}$	Upper bound β=1/10 $S_{u\text{-}ub}$	Lower bound β=1/50 $S_{u\text{-}lb}$
Crust layer	0.44	704	170	170	874	874
	0.22	352	383	454	735	806
	0	0	490*	490*	490	490
No crust	0.44	704	-	-	704	704
	0.22	352	-	-	352	352
	0	0	-	-	0	0

*corresponds to the maximum load from the crust layer

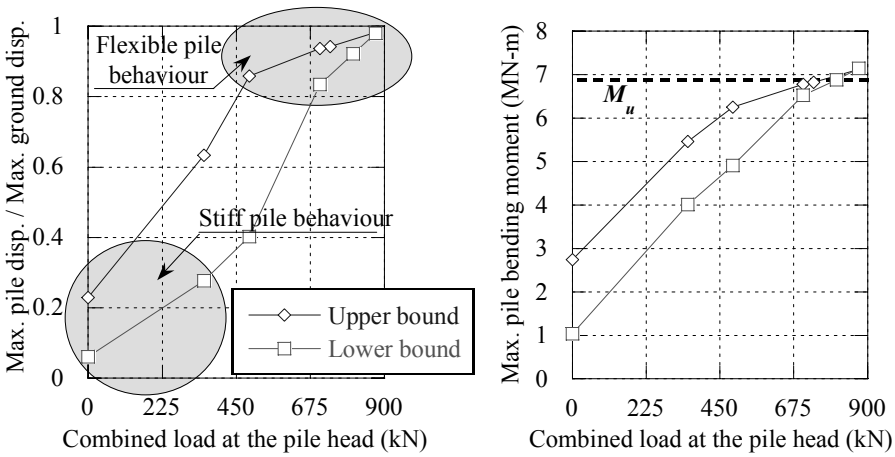

Figure 20. ***Effect of total load applied at the pile head on the peak pile displacements and bending moments for different combinations of inertial and crust layer loads, considering both relatively stiff and relatively soft liquefied soils.***

Figure 20a shows the ratio of maximum pile displacement to the maximum free field ground displacement plotted against the total load at the pile head for both the upper and lower bound cases. It can be seen that both cases show flexible pile behaviour (ratio approaches one) when large loads are applied and stiff pile behaviour (ratio approaches zero) when relatively small load is applied. However the transition between stiff and flexible differs between the upper and lower bound cases adopted in the analysis. For cases with the upper bound liquefied stiffness and strength, flexible behaviour occurs at loads that are approximately 30% less than the lower bound cases; in other words, stiffer liquefied soil results in more flexible behaviour of the pile. For the case where no inertial load is applied (the total pile load is the 490 kN from the crust layer), the upper bound case has a pile displacement twice as large as the lower bound case. These features are also observed in the maximum pile bending moments shown in Figure 20b.

When considering lateral spreading cases stiff pile behaviour is predominately observed. This is reasonable as the liquefied soil must have relatively low stiffness and strength in order for lateral spreading to occur. Due to this stiff behaviour, the relative displacement in the crust layer is likely to be large; thus the crust soil will be yielding and the maximum pressure from the crust layer will always be applied. As inertial loads during this phase are likely to be small, when evaluating the total load at the pile head attention should be focussed to considerations of variations in the passive load from the crust layer.

CONCLUDING REMARKS

Simplified analysis of pile foundations in liquefied soil is burdened by many uncertainties. In this paper a case study is presented where a parametric study was conducted to determine the effects of these uncertainties on the pile response. Key findings include:

- The effect that the stiffness and ultimate strength of liquefied soil have on pile response depends on the behaviour of the pile under loading; flexible piles have small relative displacements hence the liquefied soil properties and ultimate pressure from the crust layer have little effect, in contrast to stiff piles with large relative displacements.
- For stiff piles, the level of stiffness and strength degradation due to liquefaction adopted in the analysis had a large effect on the pile response. When lower bound values of stiffness and strength were adopted the pile showed smaller lateral displacements and bending moments as compared to those obtained in the analysis with upper bound values.
- Using equivalent linear p-δ relationships in the liquefied layers have been shown to predict overly conservative bending moments in cases where the liquefied soil is relatively stiff and the relative displacements are large. A more appropriate approach is to use a bi-linear p-δ relationship for the liquefied soil where the ultimate pressure is limited to the undrained residual strength of the soil.
- For stiff piles undergoing lateral spreading, there exists a threshold magnitude of lateral ground displacement above which any further increase in the ground displacement has no effect on the pile response. This threshold value depends on the stiffness and strength of the liquefied soil.
- Increasing the load at the pile head may lead into a transition from stiff to flexible pile behaviour. This transition occurs earlier in relatively stiff liquefied soils.

In the design of pile foundations in liquefiable soil, stiff pile behaviour is desired. Flexible piles suffer large pile displacements and often fail in bending, thus the parameters that are most important for design are those that affect stiff piles. The parametric study described in this paper suggests that the choice of liquefied soil properties adopted in design have a large bearing on the computed response for stiff piles. In contrast it was shown that once a certain magnitude of ground displacement has been reached further increases in ground displacement have no effect. Therefore in design threshold ground displacement needs to be evaluated first and then accordingly attention should be paid to the effects of the crust layer and the liquefied soil properties. The study also showed the importance of inertial loads, as the magnitude of inertial load applied has a large effect on the relative pile displacements and hence response of the pile.

REFERENCES

Architectural Institute of Japan. (2001). *Recommendations for the Design of Building Foundations*.

Chang, D., Boulanger, R. W., Brandenberg, S. J. and Kutter, B. L. (2005). "Dynamic analysis of soil-pile-structure interaction in laterally spreading ground during earthquake shaking." *ASCE Geotechnical Special Publication 145*, 218-229.

Cubrinovski, M. and Ishihara, K. (2004). "Simplified method for analysis of piles undergoing lateral spreading in liquefied soils." *Soils and Foundations*, **44**(5), 119-133.

Cubrinovski, M. and Ishihara, K. (2006). "Assessment of pile group response to lateral spreading by single pile analysis." *ASCE Geotechnical Special Publication 145*, 242-254.

Cubrinovski, M., Ishihara, K. and Kijima, T. (2001). "Effects of liquefaction on seismic response of a storage tank on pile foundations." *Fourth International Conference on Recent Advances in Geotechnical Earthquake Engineering and Soil Dynamics*.

Cubrinovski, M., Ishihara, K. and Poulos, H. (2006a). "Psuedo static analysis of piles subjected to lateral spreading." *NZ Workshop on Geotechnical Engineering*, Christchurch 2006, 337-350.

Cubrinovski, M., Kokusho, T. and Ishihara, K. (2006b). "Interpretation from large-scale shake table tests on piles undergoing lateral spreading in liquefied soils." *Soils Dynamics and Earthquake Engineering*, Vol. **26**, 275-286.

Dowrick, D. J., Berryman, K. R., McVerry, G. H. and Zhao, J. X. (1998). "Earthquake hazard in Christchurch." *Bulletin of the New Zealand National Society for Earthquake Engineering*, **31**(1), 1-22.

Hamada, M. and O'Rourke, T. D. (1992). "*Case studies of liquefaction and lifeline performance during past earthquakes.*" M. Hamada and T. D. O'Rourke, eds., National Center for Earthquake Engineering Research, Buffalo, NY.

Hatanaka, M. and Uchida, A. (1996). "Empirical correlation between penetration resistance and internal friction angle of sandy soils." *Soils and Foundations,* **36**(4), 1-9.

Idriss, I. M. and Boulanger, R. W. (2007). "SPT- and CPT-Based relationships for the residual shear strength of liquefied soils." *4th International Conference on Earthquake Geotechnical Engineering - Invited Lectures*, Thessaloniki, Greece.

Ishihara, K. and Cubrinovski, M. (1998). "Performance of large-diameter piles subjected to lateral spreading of liquefied deposits." *13th Southeast Asian Geotechnical Conference*, Taipei.

Ishihara, K. and Cubrinovski, M. (2004). "Case studies of pile foundations undergoing lateral spreading in liquefied deposits." *Fifth International Conference on Case Histories in Geotechnical Engineering*, New York.

Ishihara, K., Yoshida, K. and Kato, M. (1997). "Characteristics of lateral spreading in liquefied deposits during the 1995 Hanshin-Awaji Earthquake." *Journal of Earthquake Engineering*, **1**(1), 23-55.

Japanese Geotechnical Society. (1998). "Special Issue on Geotechnical Aspects of the January 17 1995 Hyogoken Nambu Earthquake."

Liao, S. and Whitman, R. V. (1986). "Overburden correction factors for SPT in sand." *Journal of Geotechnical Engineering - ASCE*, **112**(3), 373-377.

Liyanapathirana, D. S. and Poulos, H. G. (2005). "Pseudostatic approach for seismic analysis of piles in liquefying soil." *Journal of Geotechnical and Geoenvironmental Engineering*, **131**(12), 1480-1487.

O'Rourke, T. D., Meyersohn, W. D., Shiba, Y. and Chaudhuri, D. (1994). "Evaluation of pile response to liquefaction-induced lateral spread." Tech. Report NCEER-94-0026.

Olson, S. M. and Stark, T. D. (2002). "Liquefied strength ratio from liquefaction flow failure case histories." *Canadian Geotechnical Journal*, **39**(3), 629-647.

Orense, R., Ishihara, K., Yasuda, S., Morimoto, I. and Takagi, M. (2000). "Soil spring constants during lateral flow of liquefied ground." *12th World Conference on Earthquake Engineering*, Auckland, New Zealand.

Seed, H. B. (1987). "Design problems in soil liquefaction." *Journal of Geotechnical Engineering - ASCE*, **113**(8), 827-845.

Seed, R. B. and Harder, L. F. (1990). "SPT based analysis of cyclic pore pressure generation and undrained residual strength." *H. Bolton Seed Memorial Symposium Proceedings*, **2**, 351-376.

Stirling, M., Pettinga, J., Berryman, K. and Yetton, M. (2001). "Probabilistic seismic hazard assessment of the Canterbury region, New Zealand." *Bulletin of the New Zealand Society for Earthquake Engineering*, **34**(4), 318-334.

Tokimatsu, K. and Asaka, Y. (1998). "Effects of liquefaction induced ground displacements on pile performance in the 1995 Hyogoken-Nambu Earthquake." *Soils and Foundations* (Special Issue), 163-177.

Tokimatsu, K., Suzuki, H. and Sato, M. (2005). "Effects of inertial and kinematic interaction on seismic behavior of pile with embedded foundation." *Soil Dynamics and Earthquake Engineering*, **25**(7-10), 753-762.

Wang, S.-T. and Reese, L. C. (1998). "Design of pile foundations in liquefied soils." *ASCE Geotechnical Special Publication No. 75*, 1331-1343.

Yasuda, S. and Berrill, J. B. (2000). "Observations of the earthquake response of foundations in soil profiles containing saturated sands." *GeoEng2000*.

Youd, T. L., Hansen, C. M. and Bartlett, S. F. (2002). "Revised multilinear regression equations for prediction of lateral spread displacement." *Journal of Geotechnical and Geoenvironmental Engineering*, **128**(12), 1007-1017.

Youd, T. L., Idriss, I. M., Andrus, R. D., Arango, I., Castro, G., Christian, J. T., Dobry, R., Liam Finn, W. D., Harder L.F, Jr., Hynes, M. E., Ishihara, K., Koester, J. P., Liao, S. S. C., Marcuson III, W. F., Martin, G. R., Mitchell, J. K., Moriwaki, Y., Power, M. S., Robertson, P. K., Seed, R. B. and Stokoe II, K. H. (2001). "Liquefaction resistance of soils: Summary report from the 1996 NCEER and 1998 NCEER/NSF workshops on evaluation of liquefaction resistance of soils." *Journal of Geotechnical and Geoenvironmental Engineering*, **127**(10), 817-833.